Mon. Not. R. Astron. Soc. **000**, 000–000 (1995) Printed 9 February 1998 (MN LaTeX style file v1.3)

$UBV(RI)_{C}$ photometry and spectroscopy of the young open cluster Haffner 18 ⋆

Ulisse Munari[1] , Giovanni Carraro[2,3] and Roberto Barbon[4]

[1]*) Osservatorio Astronomico di Padova, sede di Asiago, I–36012 Asiago (VI), Italy (*munari@astras.pd.astro.it*)*
[2]*) Dipartimento di Astronomia, Universita' di Padova, vicolo dell'Osservatorio 5, I–35122, Padova ,Italy*
[3]*) SISSA/ISAS, via Beirut 2, I–34013, Trieste, Italy (*carraro@sissa.it*)*
[4]*) Osservatorio Astrofisico, I–36012 Asiago (VI), Italy (* barbon@astras.pd.astro.it *)*

Accepted....... Received.......; in original form ......

ABSTRACT

UBV(RI)$_{C}$ CCD photometry of a $2.'1 \times 3.'3$ field centered on the young open cluster Haffner 18 is presented and discussed. Spectroscopic classification of seven stars is also provided. 44 clusters members are identified, the earliest type being O6. The distance to the cluster is found to be 6.3 kpc, corresponding to a galactocentric distance of 12.7 kpc (for a Sun galactocentric distance of 8.5 kpc). Excellent fit to the observed main sequence is achieved by a solar composition isochrone of 2×10^{6} years reddened by E_{B-V}=0.62 mag. Differential reddening of intra–cluster origin is present. Pre-main sequence members are likely to be present over the 6 mag range explored by our observations (reaching down to earliest A spectral types). The presence of differential reddening and pre-main sequence members agrees with the evidence for a bright parent nebulosity embedding the whole cluster. The radial velocity of the cluster is consistent with the Hron (1987) model of galactic rotation.

Key words: Haffner 18: photometry, spectroscopy – open clusters: HR diagram.

1 INTRODUCTION

Haffner 18 ($\alpha_{2000} = 7^{h}\ 52^{m}\!.5$ $\delta_{2000} = -26^{o}\ 22'$ $l = 243^{o}\!.1$ $b = +0^{o}\!.5$) lies on the sky close to the young open cluster Haffner 19 . Both clusters are located in a region of Puppis reported by FitzGerald (1968) as remarkably free of interstellar absorption. They are therefore well suited to trace the spiral structure and galactic rotation at large distances in the general anti-center galactic direction. In this paper we present and discuss our photometric observations of Haffner 18 secured similarly to those on Haffner 19 (Munari and Carraro 1996a, hereafter MC96a) and another cluster we have previously studied in the region, Bochum 2 (Munari and Carraro 1995).

Haffner 18 was first identified by Haffner (1957) who sub–divided it into three distinct groups *a*, *b* and *c*. FitzGerald and Moffat (1974, hereafter FM) considered the two clusters Haffner 18a and 18b as a single elongated entity, parallel to the galactic plane, while the third one was interpreted as a chance alignment of field stars. FM found the cluster to be affected by differential reddening and derived a distance modulus of $(\text{m-M})_{\circ} = 14.2 \pm 0.3$. They reported the HR diagram to show evidence of pre–main sequence members, arguing for an age $T \leq 10^{6}$ yrs. FM also suggested that Haffner 18 and Haffner 19 are at the same distance and belong to spiral arm located at 15 Kpc in the anti-galactic center direction, possibly associated with the Perseus arm extension.

Labhardt et al. (1992, hereafter LSS) presented accurate CCD photometry of both Haffner 18 and 19. The systematic discrepancy with the FM data was attributed by them to different treatment of blended companions and reliable choice of the sky background. Our earlier results on Haffner 19 (MC96a) supported such a conclusion.

2 PHOTOMETRY

UBV(RI)$_{C}$ photometry of Haffner 18 has been obtained with the CCD camera on the 1.0 m telescope of the South Africa Astronomical Observatory (SAAO) at Sutherland on February 29, 1992. The same night we observed Haffner 19 on which we already reported elsewhere (MC96a). The reader is referred to Munari and Carraro (1995) for the adopted (standard) procedures and an evaluation of the excellent instrumental performances. The journal of observations is given in Table 1 and the resulting *UBV(RI)*$_{C}$ magnitudes are listed in Table 2. A finding chart is presented in Figure 1. Star #1 has been recorded very close to the CCD frame border, which caused the larger-than-average errors in Table 2. Star #52 appears resolved into two components (LSS 38 and LSS 39) by Labhardt et al. (1992). Both stars #1 and 52 will be ignored in the following. On the other hand, star FM 3067 has been resolved into two objects

⋆ Based on observations collected with the telescopes of the South African Astronomical Observatory (Sutherland, RSA) and ESO (La Silla, Chile).

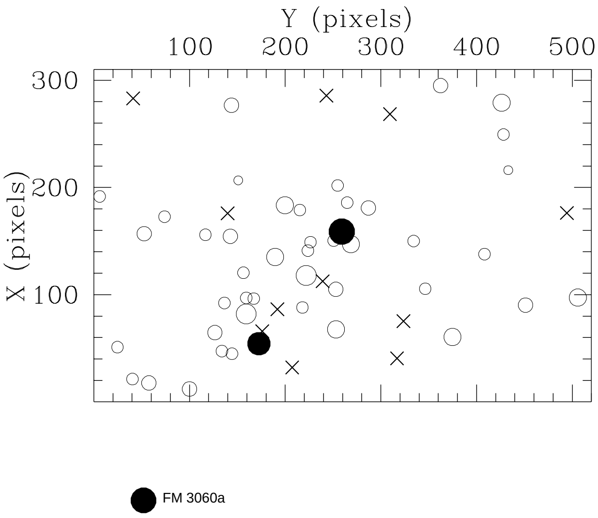

Figure 1. Finding chart for the programme stars. The CCD field cover 2.1×3.3 arcmin. North on top, East to the left. *Crosses*: field stars. *Open circles*: cluster members. *Filled circles*: the three earliest type cluster members (O7, O9 and B0.5, the latter laying outside the region covered by our observations).

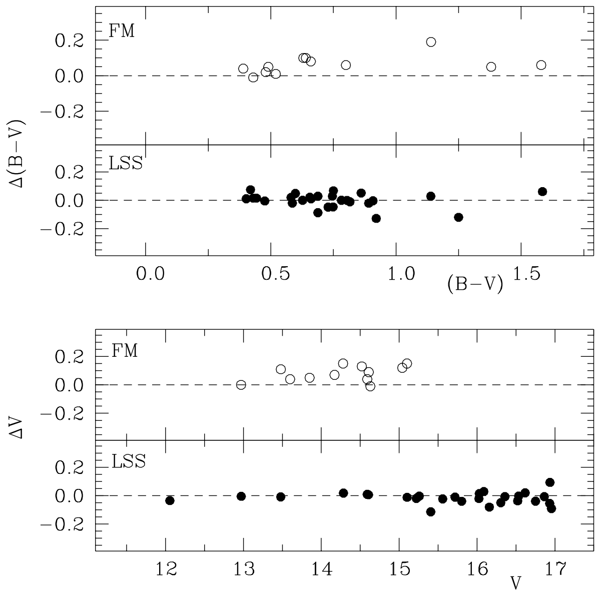

Figure 2. Comparison between FM, LSS and our photometry for the stars in common.

(#43 and 44) and FM 3081 into three (#55, 56 and 57). Values for star #53 in Table 2 are nearly identical with those given by LSS (their star 37), whilst FM data (their star 3073) are largely off. The difference is too large to be explained in term of observational errors and most probably it is due just to a printing error. For these reasons stars #53, FM 3067 and FM 3081 are not considered in the comparison with FM data in Eq.(1) and (2).

Comparison between our profile CCD photometry (performed with the DAOPHOT package) and the FM aperture photoelectric photometry for the 12 stars in common yields:

$$V - V_{FM} = 0.078 \qquad \sigma = 0.055 \qquad (1)$$

$$(B-V) - (B-V)_{FM} = 0.063 \qquad \sigma = 0.052 \qquad (2)$$

For the 27 stars in common with the profile CCD photometry by LSS (who used the ROMAPHOT package) the comparison gives:

$$V - V_{LSS} = -0.018 \qquad \sigma = 0.041 \qquad (3)$$

$$(B-V) - (B-V)_{LSS} = -0.001 \qquad \sigma = 0.051 \qquad (4)$$

Details of the comparison are given in graphical form in Figure 2. The results are fairly similar to those obtained by MC96a for Haffner 19, with aperture photometry poorly performing in a stellar field as crowded as that of Haffner 18. On the other hand the comparison with LSS photometry is quite satisfactory, with the very small residual differences easily accounted for by the different system of standard stars used (Landolt's equatorial stars for LSS, Cousins' E-regions for us) and possibly some subtle differences introduced by the reduction softwares (DAOPHOT vs. ROMAPHOT).

3 SPECTROSCOPY

Angela Bragaglia (Astronomical Observatory of Bologna) obtained for us on Feb. 25, 1994 a long list spectrum of Haffner 18 with the B&C + CCD spectrograph on the ESO 1.5 m telescope in La Silla (Chile). The covered range is λλ 3380–9190 Å, the dispersion 2.5 Å/pixel and the resolution ∼7 Å. The slit was rotated so to record on a single exposure the spectra of stars #18, 44, 52 and 56 plus stars FM 3049, 3059 and 3060a. Emission lines from the underlying nebulosity are recorded over the whole slit height (∼4 arcmin) being particularly strong around star FM 3060a. Due to different placement on the slit and different brightness, the signal–to–noise ratio of the spectra of the individual stars differs greatly, ranging from ∼80 to ∼11.

Available spectroscopic data on Haffner 18 are summarized in Table 3 (our and FM classification). Color excesses and distance moduli have been computed relative to the intrinsic colors and absolute magnitudes listed by FitzGerald (1970), Bessell (1990) and Schmidt-Kaler (1982), assuming the standard Savage & Mathis (1979) interstellar extinction law. Empty fields refer to either no available data or cases in which the interpolation between tabular reference seemed too hazardous. Input photometry for FM 3049, 3059 and 3060a comes from FM data properly shifted to our system.

Table 1. Journal of observations. *Seeing* is the FWHM of stellar images as measured on the CCD frames.

Date	Filter	Exp. time (sec)	Seeing (″)
Feb. 29, 1992	U	600	2.1
	V	22	1.9
	V	600	1.8
	B	900	1.9
	B	60	2.0
	R	10	2.1
	R	330	1.9
	I	10	1.7
	I	600	1.9

Table 2. $UBV(RI)_C$ photometry of Haffner 18. The columns give our identification number and those used by FM and LSS, the X and Y positions on the CCD frame, the magnitudes and their associated internal errors (as provided by the DAOPHOT package; in millimag). For the reasons given in the text, stars #1 and 52 have not been used in the analysis. *Asterisks*: see text. In the second column a *N* indicates a star that our analysis suggests to be a field star.

ID		FM	LSS	X	Y	V	σ_V	B-V	σ_{B-V}	V-I	σ_{V-I}	V-R	σ_{V-R}	U-B	σ_{U-B}
1		3090		231.11	–1.46	14.672	25			0.432	25	0.164	25		
2		3089		191.62	6.16	16.364	5	1.108	12	1.495	6	0.657	13		
3		3053	25	51.07	24.74	16.158	4	0.729	7	0.808	6	0.382	14		
4		3054	21	21.34	40.43	16.024	4	0.661	6	0.814	5	0.369	13		
5	N	3091		283.08	41.19	12.430	0	0.394	1	0.420	1	0.201	1	–0.024	2
6		3088	46	156.87	52.66	15.803	3	0.419	5	0.444	6	0.149	13		
7		3055	20	17.70	57.58	15.258	2	0.688	4	0.800	3	0.377	7		
8			47	172.75	73.98	16.751	13	0.816	18	0.927	15				
9		3056	19	12.09	100.01	15.102	2	0.656	4	0.796	3	0.379	5		
10			45	155.93	116.66	16.956	14	0.908	21	0.975	17				
11		3069	29	64.71	126.52	15.559	3	0.443	4	0.610	5	0.263	9		
12			34	92.29	136.54	16.933	8	0.598	13	0.804	13				
13	N	3077	48	175.85	139.75	12.972	1	1.585	2	1.641	1	0.811	1		
14		3076	44	154.47	142.70	15.717	3	0.861	5	1.171	6	0.560	9		
15				206.65	150.97	17.162	9	0.658	17	0.932	13				
16		3071	40	120.49	156.35	16.358	5	1.250	13	1.547	6	0.743	12		
17		3075	41	135.13	189.49	14.589	1	0.627	2	0.973	1	0.412	3		
18	N	3072a	32	86.51	191.84	14.284	3	0.804	4	1.064	4	0.496	4		
19	N	3066	22	32.18	207.28	14.607	1	1.139	3	1.256	1	0.599	3		
20			33	88.10	218.05	16.534	6	0.921	11	1.307	7				
21	N	3085		285.62	243.16	11.839	1	1.084	1	0.999	1	0.531	1	0.607	4
22		3065		67.69	253.10	14.631	1	0.640	2	0.665	1	0.331	3		
23		3080		201.84	254.84	16.464	5	0.530	9	0.737	9				
24				185.91	264.80	16.961	14	0.760	25	1.097	22				
25		3082		180.93	286.99	15.041	4	0.489	4	0.725	5	0.306	6		
26	N	3084		268.37	309.48	9.901	4	1.119	6	1.084	8	0.512	6	0.790	5
27	N	3064		40.56	316.85	13.850	1	0.481	1	0.563	1	0.261	2	0.063	10
28	N	3063		75.31	323.64	13.598	1	1.377	2	1.424	1	0.707	2		
29				150.04	334.21	17.000	9	0.872	15	0.937	11				
30				105.55	346.37	16.923	9	0.651	14	0.734	11				
31		3083		295.09	362.36	15.659	3	0.668	5	0.797	4	0.357	9		
32		3062		60.61	374.86	14.169	2	0.522	2	0.608	3	0.290	4		
33				137.79	408.30	16.931	10	0.739	16	0.962	21				
34		2057		279.02	426.23	14.520	1	0.583	2	0.651	2	0.302	3		
35				249.43	428.16	16.458	5	1.029	10	1.410	5	0.690	14		
36				216.13	433.09	17.118	9	0.631	16	0.742	13				
37				90.30	451.13	15.925	3	0.632	6	0.758	4	0.350	12		
38	N			176.22	494.45	13.720	1	0.594	1	0.706	1	0.335	2	0.112	10
39				97.33	505.83	14.594	1	0.589	2	0.685	2	0.406	59		
40		3068	24	47.38	133.86	16.305	12	0.581	19	0.798	18				
41			23	44.94	144.39	16.522	18	0.586	25	0.931	27				
42		3086		276.67	143.90	15.701	3	0.387	4	0.413	5				
43		3067*	27	54.34	172.59	12.055	1	0.402	2	0.598	3	0.263	1	–0.559	2
44	N	3067*	28	62.83	175.97	15.406	6	0.688	23			0.072	18		
45		3078		183.46	199.76	14.517	2	0.391	3	0.584	2	0.241	4	–0.380	2
46		3079	49	178.95	215.35	16.029	7	0.476	9	0.546	9	0.229	16		
47			42	141.11	223.74	16.618	7	0.782	12	0.890	9				
48			43	148.99	226.47	16.864	9	0.749	17	1.177	11				
49		3070	31	82.09	159.24	13.479	1	0.429	1	0.603	1	0.260	2	–0.443	4
50			36	96.98	159.33	16.087	6	0.746	9	0.844	8	0.417	25		
51			35	96.38	167.13	16.936	14	0.750	24	0.906	19				
52		3074	38,39*	117.96	221.94	13.025	1	0.158	3	0.250	5	0.093	2	–0.236	5
53	N	3073	37	112.51	239.13	15.220	3	0.891	11	1.096	4	0.590	12		
54		3072b		105.03	252.90	15.624	3	0.468	5	0.833	4	0.465	9		
55		3081*		150.43	250.66	16.153	20	0.546	33	0.991	33				
56		3081*		158.83	259.14	11.212	1	0.333	3	0.453	2	0.183	1	–0.634	3
57		3081*		147.11	268.75	14.933	8	0.769	14	0.967	9	0.527	12		

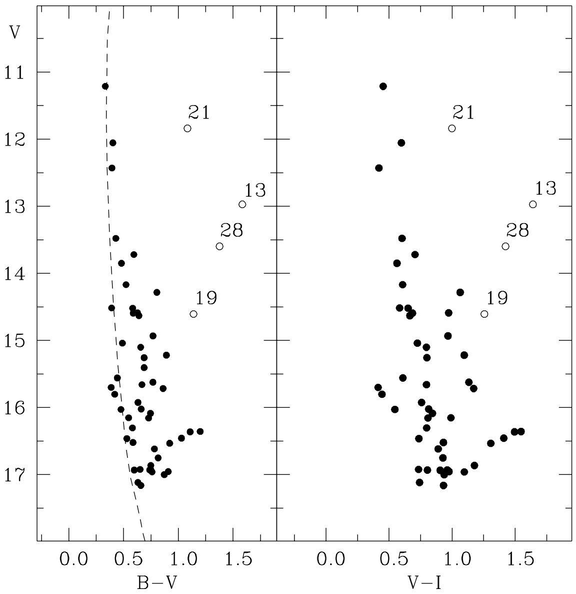

Figure 3. *V-(B-V)* and *V-(V-I_C)* color magnitude diagrams from Table 2. Probable field stars are labeled. The dotted line is a solar abundance $T = 2 \times 10^6$ yr isochrone from the Padova group (Bertelli et al. 1994).

4 RESULTS

4.1 Color-Magnitude diagram

The *V-(B-V)* and *V-(V-I_C)* diagrams are shown in Figure 3. The main sequence appears well defined down to the limit of our photometry in Table 2 (V = 17.2 mag). Star #26 (a G8 V) is clearly a foreground object (cf. Table 3) and lies outside the diagram limits in Figure 3. Labeled stars (#13, 19, 21 and 28) are classified as field stars from their location in the color-magnitude diagrams. It has also to be noted that according to the preliminary spectroscopic results of Table 3 stars #18 and 44 are not members if their luminosity class is taken to be V.

Our *V-(B-V)* and *V-(V-I_C)* diagrams are affected by errors not exceeding σ=0.015 mag over the explored range, and therefore the widening of the main sequence with fainter magnitudes is a real effect that we ascribed to the combined effects of differential reddening and presence of pre–main sequence stars. Similar conclusions were reached by FM. A few field stars could be still hidden in the cluster main sequences of Figure 3. We secured photometry for a couple of field regions around Haffner 18 to the aim of statistically clean the diagrams in Figure 3. However, the strong intra–cluster extinction, reddening and emission nebulosity prevent our attempt to perform the exercise in a straightforward manner.

4.2 Distance, Reddening and Age

Distance modulus and mean reddening have been obtained through trial fits to the observed color-magnitude diagram with theoretical isochrones of the Padova group (*cf.* Bertelli *et al.* 1994) characterized by a standard [He/H] ratio and Z=0.020.

To better estimate distance and color excess of Haffner 18 we fitted in Figure 3 the locus of main sequence stars with minimal reddening. The fit is good over the whole blue side of the main sequence, particularly for the O stars on the upper sequence. Their stronger winds could have already blown away from their surroundings the residuals of the parent cloud, thus reducing towards pure interstellar terms the reddening affecting them.

The best fit is achieved for an age $T = 2 \times 10^6$ yrs, a reddening $E_{B-V} = 0.62 \pm 0.08$ and a distance modulus (m-M)$_\circ = 14.0 \pm 0.2$ mag (corresponding to a distance of 6.3 kpc). This is fairly compatible with the average spectroscopic distance modulus of the four OB stars in Table 3 which is (m-M)$_\circ = 14.57 \pm 0.94$ mag. FM estimated from fit to their ZAMS a value (m-M)$_\circ = 14.2 \pm 0.3$ mag. The three determinations well agree inside the errors. Comparison with the results by MC96a suggests that Haffner 18 and Haffner 19 are located at significantly different distances, appearing close on the sky just by chance alignment. FM on the contrary argued for Haffner 18 and 19 to lay close in space.

The $Q-$method (Becker 1963) has been applied to the stars in Table 2 with U band photometry available. The resulting reddening free color-magnitude diagram is presented in Figure 4. Star #53 and FM 3060a have been also plotted, their de–reddened values inferred from the spectroscopy in Table 3. The excellent fit to a 2×10^6 yrs isochrone scaled to (m-M)$_\circ = 14.0$ mag is evident as well the segregation of several field stars. The location of star FM 3060a cannot be reconciled with the B1 V classification by FM, its position being in excellent agreement with the B0.5 III classification given in Table 3.

The mean reddening for the cluster members in Figure 4 (the O-B earliest members) is $E_{B-V} = 0.66 \pm 0.03$. Another way to estimate the *mean* reddening over the cluster (thus including the differential reddening) is through a linear fit to the main sequence in the B–V, B–I_C plane as suggested by Natali et al. (1994) and revised by Munari and Carraro (1996b). Since this method applies only to main sequence stars, we tried to avoid pre main sequence objects by using only those stars that in Figure 3 lie closer than $\triangle B-V$=0.15 to the fitting isochrone. The linear fit on the B–V, B–I_C plane (see Figure 5) as described by Munari and Carraro (1996b) for the R$_V$=3.1 extinction law

$$(B-I) \;=\; \Omega \;+\; 2.25(B-V) \tag{5}$$

leads to the following expression for the color excess:

$$E_{B-V} = \frac{\Omega - 0.014}{0.159} \tag{6}$$

The fit in Figure 5 gives Ω=0.129 which implies E$_{B-V}$=0.72, close to the mean value over the cluster E$_{B-V}$=0.70 reported by FM and in fair agreement with the above derived values (0.62 and 0.66).

4.3 Membership

We have surveyed 57 stars in a region $2.1' \times 3.3'$ roughly centered on the cluster core. Excluding stars #1 and #52 for the reasons given above, among the remaining 55 stars we have above identified 11 non-members (marked with an N in the second column of Table 2). The remaining 44 stars are taken as cluster members once differential reddening and pre–main sequence objects are taken into account.

4.4 Galactic rotation

FM have reported preliminary radial velocities for three stars of Haffner 18. Dropping star FM 3081 which is probably a binary (FM suspected the spectrum to be doubled–lined), the remaining two stars give a heliocentric radial velocity of $\sim 67 \pm 10$ km sec^{-1} for Haffner 18. FM reported that this velocity gives a kinematic distance of 4.5 kpc based on the Schmidt (1965) rotation model of

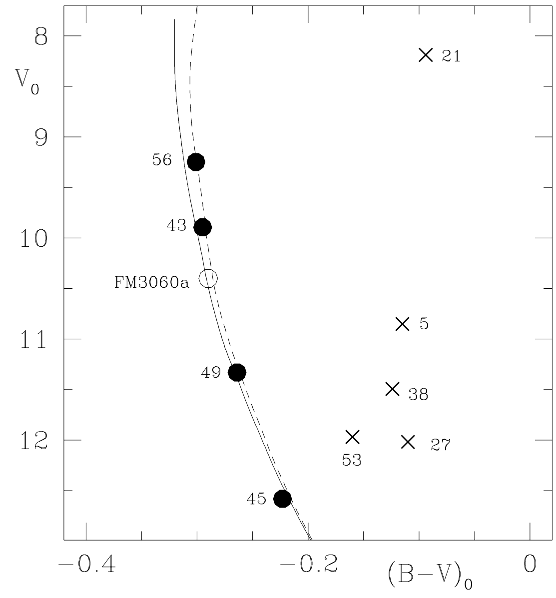

Figure 4. Location on the $V_\circ$-$(B$-$V)_\circ$ diagram of the programme stars with available U band photometry de reddened via the Q–method. Field stars are indicated with crosses. The solid and dashed lines are the ZAMS and a solar abundance 2×10^6 yr isochrone from the Padova group (Bertelli et al. 1994), scaled to (m-M)$_\circ$ = 14.0 mag.

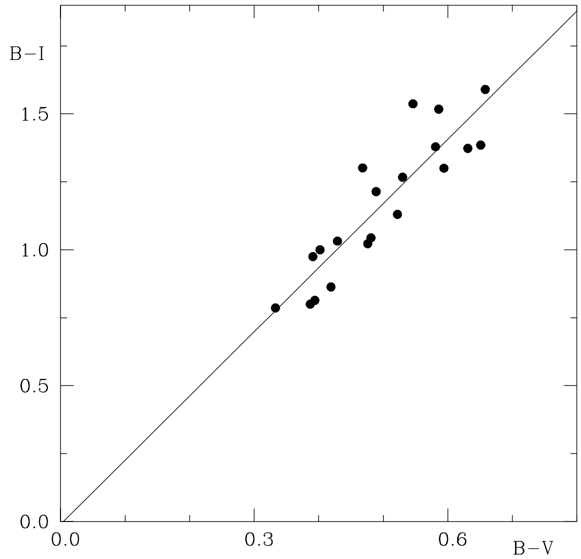

Figure 5. Haffner 18 members plotted on the (B-V)-(B-I_C) plane. The solid line is the least square fit described in sect. 4.2

the Galaxy, which is significantly shorter than 6.9 kpc distance they derived from fitting to the ZAMS.

The heliocentric component of the cluster radial velocity due to the galactic rotation can be expressed as:

$$RV_\odot \;=\; w_\circ \sin b + u_\circ \cos l \cos b + v_\circ \sin l \cos b - 2[A(R-R_\circ)+\alpha(R-R_\circ)^2] \sin l \cos b \qquad (7)$$

where as usual A denotes the Oort's constant, α is the curvature term (cf. Hron 1987), R,R$_\circ$ are the cluster and Sun galactocentric distances, d the cluster–Sun distance, (l,b) the heliocentric galactic coordinates of the cluster and $(u_\circ, v_\circ, w_\circ)$ is the solar motion vector. Adopting our estimate of 6.3 kpc for the distance and $(u_\circ, v_\circ, w_\circ)$=(9.3,11.2,7.0) km sec^{-1} from Pont et al. (1994), Eq.(7) rewrites for Haffner 18 as:

$$RV_\odot \;=\; -14.1 + 7.4A + 31.0\alpha \qquad (8)$$

Hron (1987) has used distances and radial velocities to young open clusters to investigate the rotation curve of the Galaxy. His results valid for the range $-3 < R - R_\circ < 5$ kpc are best fitted by A=17.0$\pm$ 1.5 km sec^{-1} kpc^{-1} and $\alpha = -2.0 \pm 0.6$ km sec^{-1} kpc^{-2}. If we insert them in Eq.(8) the radial velocity of Haffner 18 results to be 50 km sec^{-1}, which marginally agrees inside the errors with the $\sim 67 \pm 10$ km sec^{-1} given by FM. To obtain exactly 67 km sec^{-1} from the Hron's rotation curve it is enough to lower the curvature term to $\alpha = -1.44$, a value well compatible with the uncertainty given by Hron.

In this sector of the galactic plane the radial component of the galactic motion is however not very sensitive to the Sun–cluster distance. We may nevertheless conclude that there is no discrepancy between the photometric, spectroscopic and kinematic independent determinations of the distance to Haffner 18.

Table 3. Spectroscopic classification, reddening and spectroscopic parallaxes. *FM*: numbering and classification from Fitzgerald and Moffat (1974). See sect. 2 for a warning on star #52.

this paper		FM		E_{B-V}	E_{U-B}	E_{V-R}	E_{V-I}	(m-M)$_\circ$
18	A4	3072a		0.68		0.45	0.95	10.4
26		3084	G8 V	0.38	0.49	0.08	0.27	3.2
43		3067	O9 IV	0.71	0.57	0.42	0.93	15.1
44	A5–6			0.53		0.01		11.6
52	A0 II/III	3074						
53		3073	B5:	1.05		0.62	1.19	13.2
56	O6	3081	O7:	0.65	0.55	0.34	0.78	14.7
	F0 II:	3049		0.25	0.0			17.9
	A2	3059		0.14	0.03			12.8
	B0.5 III	3060a	B1 V	0.50	0.33			15.3

ACKNOWLEDGMENTS

One of us (UM) was Visiting Astronomer at the South African Astronomical Observatory (Cape Town) when the observations described in this paper were collected. This work has been financially supported by the Italian Ministry of University, Scientific Research and Technology (MURST) and the Italian Space Agency (ASI).

REFERENCES

Bertelli G., Bressan A., Chiosi C., Fagotto F., Nasi E., 1994, A&AS 106, 275
Becker W. 1963, in Stars and Stellar Systems: Basic Astronomical Data, K.A.Strand ed., Univ. of Chicago Press, pag. 241
Bessell M. S., 1990, PASP 102, 1181
FitzGerald M. P., 1968, A. J. 73, 983
FitzGerald M. P., 1970 A&A 4, 234
FitzGerald M. P., Moffat A. F. J., 1974, AJ 79, 873 (FM)
Haffner H., 1957, Z.f.Astrophysik 43, 89
Hron J., 1987, A&A 176, 34
Labhardt L., Spaenhauer A., Schwengeler H., 1992, A&A 265, 869 (LSS)

Munari U., Carraro G., 1995, MNRAS 277, 1269
Munari U., Carraro G., 1996a, MNRAS 283, 905 (MC96a)
Munari U., Carraro G., 1996b, A&A 314, 108
Natali F., Natali G., Pompei E., Pedichini F., 1994, A&A 289, 756
Pont F., Mayor M, Burki G., 1994, A&A 285, 415
Savage B.D., Mathis J.S. 1979, ARA&A 17, 73
Schmidt M. 1965, in *Stars and Stellar Systems: Galactic Structure*, ed. A. Blaauw and M. Schmidt, Univ. of Chicago Press, p. 513
Schmidt-Kaler, Th. 1982 in Landolt-Börnstein, Numerical Data and Functional Relationships in Science and Technology, ed. K.Schaifer & H.H. Voigt, New Series, Group IV, Vol.II(b) (Pringer, Berlin), pag. 14